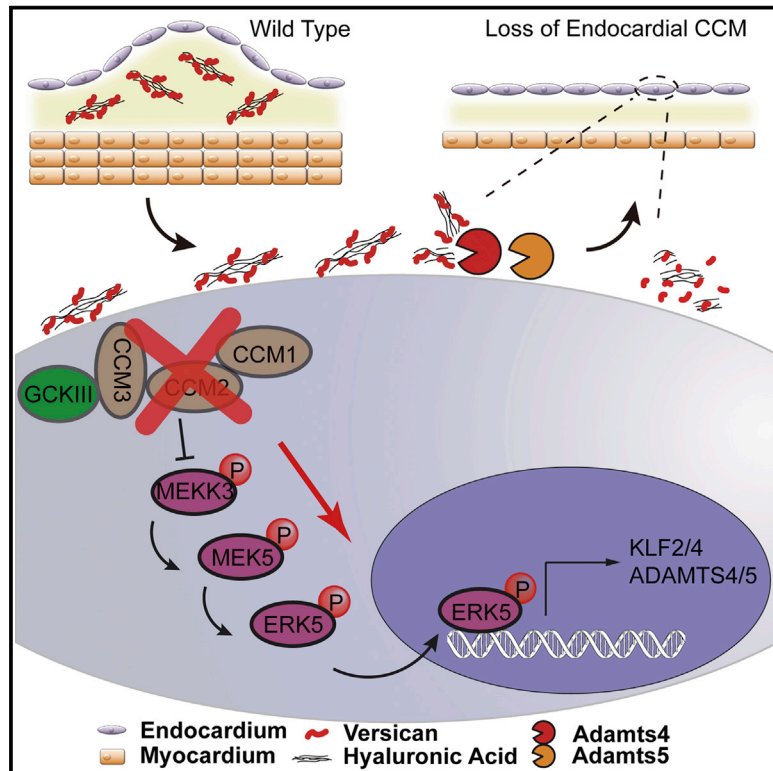# Developmental Cell

The Cerebral Cavernous Malformation Pathway Controls Cardiac Development via Regulation of Endocardial MEKK3 Signaling and KLF Expression

Graphical Abstract

Highlights

- Endocardial CCM signaling regulates cardiac jelly during heart development

- CCM signaling controls endothelial KLF and ADAMTS gene expression

- MEKK3 signaling controls endothelial KLF and ADAMTS expression in response to flow

- CCM signaling regulates endothelial gene expression through the MEKK3 pathway

Authors

Zinan Zhou, David R. Rawnsley, ..., Xiangjian Zheng, Mark L. Kahn

Correspondence

x.zheng@centenary.org.au (X.Z.),
markkahn@mail.med.upenn.edu (M.L.K.)

In Brief

The cerebral cavernous malformation pathway is necessary for cardiovascular development and to prevent vascular malformations later in life. How this pathway regulates endothelial cell function remains unclear. Zhou et al. demonstrate that CCM signaling inhibits the MEKK3 signaling pathway to control endothelial gene expression during cardiovascular development.

CrossMark

CellPress

The Cerebral Cavernous Malformation Pathway Controls Cardiac Development via Regulation of Endocardial MEKK3 Signaling and KLF Expression

Zinan Zhou,[1,8] David R. Rawnsley,[1,8] Lauren M. Goddard,[1] Wei Pan,[1] Xing-Jun Cao,[2] Zoltan Jakus,[1,9] Hui Zheng,[1] Jisheng Yang,[1] J. Simon C. Arthur,[3] Kevin J. Whitehead,[4] Dean Li,[4,5] Bin Zhou,[6] Benjamin A. Garcia,[2] Xiangjian Zheng,[1,7,*] and Mark L. Kahn[1,*]

[1]Department of Medicine and Cardiovascular Institute, University of Pennsylvania, 3400 Civic Center Boulevard, Philadelphia, PA 19104, USA
[2]Department of Biochemistry and Biophysics, University of Pennsylvania, 3400 Civic Center Boulevard, Philadelphia, PA 19104, USA
[3]Division of Cell Signaling and Immunology, University of Dundee, Dundee DD1 5EH, UK
[4]Division of Cardiovascular Medicine and the Program in Molecular Medicine, University of Utah, Salt Lake City, UT 84112, USA
[5]The Key Laboratory for Human Disease Gene Study of Sichuan Province, Institute of Laboratory Medicine, Sichuan Academy of Medical Sciences & Sichuan Provincial People's Hospital, Chengdu, Sichuan 610072, China
[6]Department of Genetics, Pediatric, and Medicine (Cardiology) and Wilf Cardiovascular Research Institute, Albert Einstein College of Medicine of Yeshiva University, 1301 Morris Park Avenue, Bronx, NY 10461, USA
[7]Lab of Cardiovascular Signaling, Centenary Institute, Sydney NSW 2050, Australia
[8]Co-first author
[9]Present address: MTA-SE Lendulet Lymphatic Physiology Research Group of the Hungarian Academy of Sciences and the Semmelweis University, 1094 Budapest, Hungary
*Correspondence: x.zheng@centenary.org.au (X.Z.), markkahn@mail.med.upenn.edu (M.L.K.)
http://dx.doi.org/10.1016/j.devcel.2014.12.009

SUMMARY

The cerebral cavernous malformation (CCM) pathway is required in endothelial cells for normal cardiovascular development and to prevent postnatal vascular malformations, but its molecular effectors are not well defined. Here we show that loss of CCM signaling in endocardial cells results in midgestation heart failure associated with premature degradation of cardiac jelly. CCM deficiency dramatically alters endocardial and endothelial gene expression, including increased expression of the _Klf2_ and _Klf4_ transcription factors and the _Adamts4_ and _Adamts5_ proteases that degrade cardiac jelly. These changes in gene expression result from increased activity of MEKK3, a mitogen-activated protein kinase that binds CCM2 in endothelial cells. MEKK3 is both necessary and sufficient for expression of these genes, and partial loss of MEKK3 rescues cardiac defects in CCM-deficient embryos. These findings reveal a molecular mechanism by which CCM signaling controls endothelial gene expression during cardiovascular development that may also underlie CCM formation.

INTRODUCTION

Embryonic heart growth requires the coordinated expansion and patterning of two major cell types: endothelial cells that line the lumen of the cardiac chambers, and contractile myocardial cells that pump blood. These cell types support and interact with each other through secreted factors, i.e., endocardial-

secreted growth factors such as neuregulin and fibroblast growth factors (FGFs) that stimulate myocardial proliferation (Gassmann et al., 1995; Lavine et al., 2005) and myocardial-derived factors such as angiopoietin (Jeansson et al., 2011) that support endocardial growth. Loss of endocardial-myocardial signaling results in a failure of cardiac growth and embryonic lethality (Gassmann et al., 1995). Similar phenotypes arise in human patients with cardiac non-compaction (Jenni et al., 1999).

During the early, most rapid period of cardiac growth (embryonic day 8.5 [E8.5]–E14.5 in the mouse), abundant extracellular matrix known collectively as cardiac jelly separates the endocardium and myocardium (Nakamura and Manasek, 1981). Cardiac jelly consists of glycoaminoglycans such as hyaluronic acid (HA), and HA-binding proteins such as versican. Loss of either HA synthase or versican results in a thin myocardium that fails to proliferate and form normal trabeculae (Camenisch et al., 2000; Yamamura et al., 1997). As the heart matures and trabeculation is completed, cardiac jelly is lost and myocardial proliferation slows. Recent genetic studies in mice have implicated endocardial expression of secreted proteases such as ADAMTS1 and ADAMTS5 that degrade versican in the regulation of cardiac jelly and heart valve formation (Dupuis et al., 2011; Stankunas et al., 2008), but the upstream signaling pathways that control endothelial expression of such proteases and thereby regulate cardiac growth remain largely unknown.

The cerebral cavernous malformation (CCM) signaling pathway was discovered through genetic studies of human patients with familial vascular malformations (Chan et al., 2010; Riant et al., 2010). These studies have identified loss of function mutations in three genes, _KRIT1_, _CCM2_, and _PDCD10_ (reviewed in Riant et al., 2010) that encode intracellular adaptor proteins that associate to form a biochemical complex with the transmembrane protein Heart of Glass (HEG1) (Kleaveland et al., 2009; Zheng et al., 2010). Conditional deletion studies in mice have demonstrated that KRIT1 and CCM2 are required in

endothelial cells for branchial arch artery formation at E8.5–E9 (Whitehead et al., 2004, 2009; Zheng et al., 2010), and to prevent CCM formation in the CNS of postnatal animals (Boulday et al., 2011; Chan et al., 2011; McDonald et al., 2011). How CCM signaling regulates endothelial and vascular function remains unclear. Cell culture studies and pharmacologic studies in mice have linked CCM signaling to negative regulation of RhoA activity (Glading et al., 2007; Stockton et al., 2010; Whitehead et al., 2009; Zheng et al., 2010) and TGFb (Maddaluno et al., 2013), but definitive evidence for a causal relationship to these pathways or other downstream CCM effectors that clearly explain the pathway's function in vascular development and maintenance has been lacking.

A role for CCM signaling in the developing heart was first revealed by zebrafish embryos lacking *heg1*, *krit1*, *ccm2*, and *pdcd10* that exhibited a characteristic dilated heart phenotype (Mably et al., 2003, 2006; Zheng et al., 2010). In the developing mouse, *Heg* is strongly expressed in the endocardium and its loss results in patchy areas of thin myocardium and cardiac rupture in late gestation (Kleaveland et al., 2009; Zheng et al., 2012). We have also recently identified a CCM2 ortholog, CCM2L, that is expressed selectively in the endocardium of the developing heart where it regulates cardiac growth (Zheng et al., 2012). A major impediment to defining the role of the CCM pathway in cardiac development in mice has been early lethality due to vascular defects that prevent blood circulation. In the present study, we use an *Nfatc1^{Cre}* allele to delete CCM pathway genes specifically in the endocardium and bypass this vascular requirement (Wu et al., 2012). We find that loss of endocardial CCM signaling results in embryonic heart failure and reduced myocardial growth that is characterized by loss of cardiac jelly and preserved expression of endocardial growth factors. This phenotype is caused by increased expression of the *Klf2* and *Klf4* transcription factors and the *Adamts4* and *Adamts5* proteases that degrade the cardiac jelly protein versican. CCM-deficient endothelial gene expression changes are associated with increased activity of the MEKK3 signaling pathway, and CCM-deficient changes in cultured endothelial cells and embryonic mouse and fish hearts are rescued by reduced MEKK3 expression or activity. These studies define regulation of MEKK3 signaling and endothelial gene expression as a conserved mechanism by which CCM signaling functions in the developing heart, and raise the possibility that loss of this molecular regulatory mechanism may also participate in CCM formation.

RESULTS

Nfatc1^{Cre} Drives Recombination in the Endocardium but Not in the Endothelium of Developing BAAs or Peripheral Vessels

Previous studies of global and endothelial-specific loss of *Krit1* and *Ccm2* revealed embryonic lethality at E8.5–E9.5 due to a lack of lumenized branchial arch arteries (BAAs) and blood circulation (Boulday et al., 2009; Whitehead et al., 2004, 2009; Zheng et al., 2010), a severe vascular phenotype that was also observed in zebrafish embryos lacking HEG-CCM signaling (Zheng et al., 2010). Cardiac defects, such as atrial enlargement, reduced trabeculation, and pericardial edema, were noted in deficient mouse embryos (Boulday et al., 2009; Whitehead

et al., 2004), but because these changes arose in animals with complete vascular disruption, it was not clear if they were primary or secondary phenotypes.

To circumvent the early requirement for CCM signaling in the BAA endothelium and investigate the role of CCM signaling specifically in the heart, we used *Nfatc1^{Cre}* mice (Wu et al., 2012). Consistent with published studies, lineage tracing studies in *Nfatc1^{Cre}*;R26R-YFP animals revealed *Nfatc1^{Cre}* activity throughout the atrial and ventricular endocardium, but not in the endothelium of the distal aortic sac or the developing BAAs at E10.5 (Figures S1A–S1F available online). *Nfatc1^{Cre}* activity was observed in endothelial cells of the ascending aorta and proximal pulmonary arteries at E14.5, but not in more distal great vessels at that time point (Figures S1G–S1K) or in the endothelial cells of the peripheral vasculature in the liver or kidney at P1 (Figures S1L–S1R). These studies suggested that *Nfatc1^{Cre}* could be used to test the requirement for CCM signaling specifically within the endocardium of the developing heart.

Endocardial Deletion of *Krit1* Results in Mid-Gestation Heart Failure Associated with Loss of Cardiac Jelly

Analysis of *Nfatc1^{Cre}*;*Krit1^{fl/+}* × *Krit1^{fl/fl}* crosses at postnatal day 0.5 (P0.5) revealed that *Nfatc1^{Cre}*;*Krit1^{fl/fl}* mice die prior to birth (Table S1). Timed matings demonstrated live *Nfatc1^{Cre}*;*Krit1^{fl/fl}* embryos that were grossly indistinguishable from littermate controls at E12.5 (Figure S2), but all *Nfatc1^{Cre}*;*Krit1^{fl/fl}* embryos were dead by E14.5–E15.5 (Figure S2 and Table S1). Thus endocardial loss of KRIT1 results in embryonic lethality during mid-gestation.

To understand the cause of lethality, *Nfatc1^{Cre}*;*Krit1^{fl/fl}* and control littermates were examined at E10.5 and E12.5, time points prior to lethality. Hematoxylin and eosin staining (H&E) of *Nfatc1^{Cre}*;*Krit1^{fl/fl}* hearts at E10.5 revealed thin myocardium and smaller myocardial trabeculae compared with littermate controls, despite the presence of abundant endocardial cells (Figures 1A and 1B). These changes were more marked at E12.5, when control hearts had developed a thicker compact myocardium and well-developed trabeculae (Figures 1C and 1D). Atrial and ventricular chamber dilatation, like that observed in ccm-deficient zebrafish embryos (e.g., Figure 4 and Mably et al., 2003, 2006), were also observed in *Nfatc1^{Cre}*;*Krit1^{fl/fl}* embryos at E12.5 (e.g., Figure 1C versus Figure 1D). Most striking was the reduction in space between the endocardium and myocardium that is occupied by cardiac jelly in *Nfatc1^{Cre}*;*Krit1^{fl/fl}* embryo hearts at E10.5 and E12.5 (Figures 1A–1D). This phenotype was particularly evident in the trabeculae, where the myocardium was wrapped tightly by endocardium in the *Nfatc1^{Cre}*;*Krit1^{fl/fl}* heart but clearly separated from the endocardium in control hearts at these time points (arrows, Figures 1A–1D). Quantitation of the area occupied by cardiac jelly in the trabeculae of the E10.5 heart revealed a >65% decrease in *Nfatc1^{Cre}*;*Krit1^{fl/fl}* hearts compared with either *Krit1^{fl/fl}* or *Nfatc1^{Cre}*;*Krit1^{fl/+}* littermate hearts (Figure 1E).

The loss of endocardial-myocardial separation in *Nfatc1^{Cre}*;*Krit1^{fl/fl}* hearts suggested that endocardial loss of CCM1 results in reduced cardiac matrix/jelly. Consistent with this observation, Alcian blue staining demonstrated loss of matrix glycosaminoglycans in the *Nfatc1^{Cre}*;*Krit1^{fl/fl}* heart, particularly surrounding the trabeculae at E10.5 (Figures 1F and 1G). Versican is the major
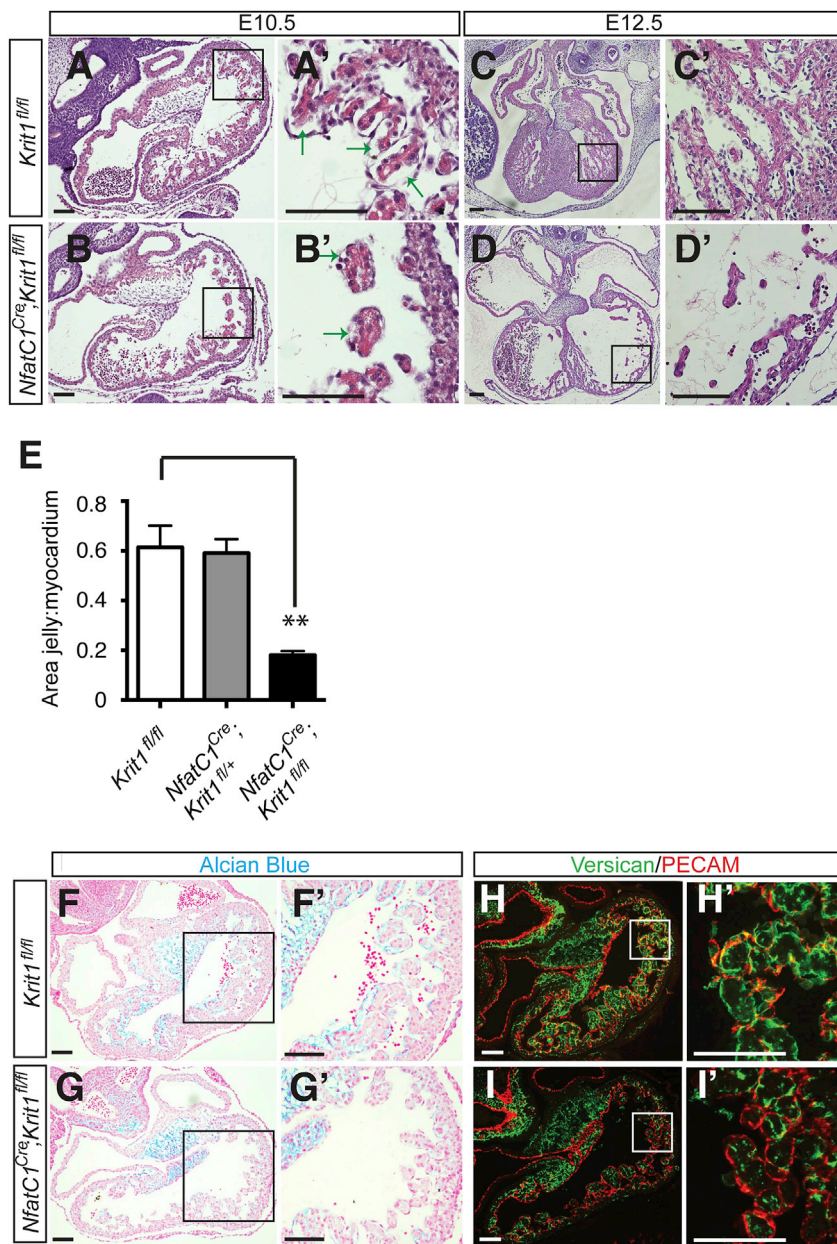
Figure 1. Lack of Endocardial *Krit1* Results in Loss of Cardiac Jelly

(A–D) *Nfatc1^{Cre};Krit1$^{fl/fl}$* hearts exhibit thinned myocardium and reduced space between endocardial and myocardial cells at E10.5 and E12.5. Arrows indicate the endocardial-myocardial gap. (A'-D') Higher magnification images of the regions boxed in (A)–(D).

(E) Ratio of the area occupied by cardiac jelly to that occupied by myocardium in the trabeculae of E10.5 littermate hearts. N = 3 embryos; nine sections analyzed for each group. **$p < 0.01$. Error bars represent SEM.

(F and G) Reduced Alcian blue staining in *Nfatc1^{Cre};Krit1$^{fl/fl}$* hearts at E10.5. (F' and G') Higher magnification images of the regions boxed in (F) and (G).

(H and I) Immunostaining for versican in *Nfatc1^{Cre};Krit1$^{fl/fl}$* and control hearts at E10.5. (H' and I') Higher magnification images of the regions boxed in (H) and (I). Scale bars represent 100 μm.

et al., 2009, 2011; Whitehead et al., 2004, 2009). However, KRIT1 also regulates integrin affinity through its interaction with ICAP1 (Liu et al., 2013) and binds RAP1 (Serebriiskii et al., 1997). Thus, the role of KRIT1 in the endocardium of the developing heart might not simply reflect the role for CCM signaling in that cell type. To test whether the cardiac abnormalities described above arise due to loss of canonical CCM signaling in the endocardium, we deleted *Ccm2* and *Pdcd10* in the endocardium using *Nfatc1^{Cre}*. *Nfatc1^{Cre};Ccm2$^{fl/fl}$* embryos exhibited embryonic lethality at the same time point as observed for *Nfatc1^{Cre};Krit1$^{fl/fl}$* embryos (Table S1). *Nfatc1^{Cre};Ccm2$^{fl/fl}$* embryos also exhibited similar reductions in cardiac jelly, myocardial growth, Alcian blue staining, and cardiac versican at both E10.5 (Figures 2A–2F) and E12.5 (Figures 2G–2L). *Nfatc1^{Cre};Pdcd10$^{fl/fl}$* embryos exhibited embryonic lethality that was later than that as observed for *Nfatc1^{Cre}; Krit1$^{fl/fl}$* and *Nfatc1^{Cre};Ccm2$^{fl/fl}$* embryos (Table S1). *Nfatc1^{Cre}; Pdcd10$^{fl/fl}$* embryos did not appear abnormal at E10.5, but reduced cardiac jelly, myocardial growth, Alcian blue staining, and versican were observed at E12.5 (Figures 2M–2R), consistent with a milder presentation of the same phenotype. These findings suggest that all three primary components of the CCM signaling pathway function in the mid-gestation endocardium to maintain cardiac jelly and support cardiac growth.

protein component of cardiac jelly, and loss of versican results in reduced myocardial growth and failure to form myocardial trabeculae. Immunostaining revealed a severe loss of intact versican in the E10.5 *Nfatc1^{Cre};Krit1$^{fl/fl}$* heart compared with controls (Figures 1H and 1I). Thus endocardial loss of KRIT1 results in mid-gestation heart failure associated with reduced cardiac jelly.

Endocardial Loss of *Ccm2* and *Pdcd10* Also Results in Loss of Cardiac Jelly

In the CCM signaling pathway, KRIT1 binds CCM2 and CCM2 binds PDCD10 to form a ternary complex (Hilder et al., 2007; Zawistowski et al., 2005; Zhang et al., 2007), and deficiency of any of these three proteins results in CCM formation in human patients and in mouse models of postnatal endothelial deficiency (Boulday

Endocardial Loss of KRIT1 Is Associated with Changes in the Expression of KLF2/4 Transcription Factors and ADAMTS4/5 Proteases

The thin myocardium and reduced cardiac jelly observed in *Nfatc1^{Cre};Krit1$^{fl/fl}$* hearts could result from reduced endocardial
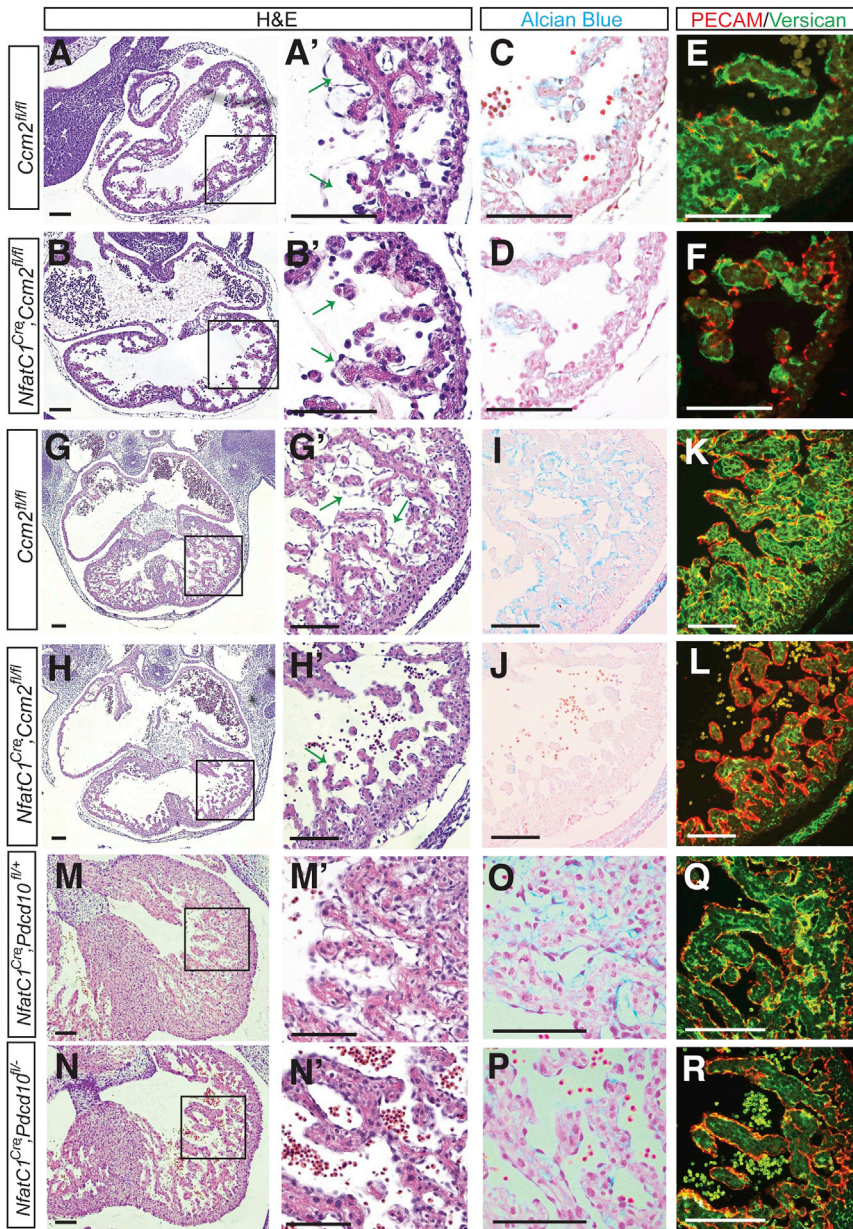
Figure 2. Endocardial Loss of *Ccm2* or *Pdcd10* Also Results in Reduced Cardiac Jelly

(A and B) Thin myocardium and reduced endocardial-myocardial space in *Nfatc1*[Cre];*Ccm2*^{fl/fl} hearts at E10.5. (A′ and B′) Higher magnification images of the regions boxed in (A) and (B). (B) Error bars represent SEM.

(C and D) Reduced Alcian blue staining in *Nfatc1*[Cre];*Ccm2*^{fl/fl} hearts at E10.5. Error bars represent SEM.

(E and F) Reduced intact versican in in *Nfatc1*[Cre];*Ccm2*^{fl/fl} hearts at E10.5.

(G and H) Thin myocardium and reduced endocardial-myocardial space in *Nfatc1*[Cre];*Ccm2*^{fl/fl} hearts at E12.5. (G′ and H′) Higher magnification images of the regions boxed in (G) and (H).

(I and J) Reduced Alcian blue staining in *Nfatc1*[Cre];*Ccm2*^{fl/fl} hearts at E12.5. (J) Error bars represent SEM.

(K and L) Reduced intact versican in in *Nfatc1*[Cre];*Ccm2*^{fl/fl} hearts at E12.5. (K) Error bars represent SEM.

(M and N) Thin myocardium and reduced endocardial-myocardial space in *Nfatc1*[Cre];*Pdcd10*^{fl/fl} hearts at E12.5. (M′ and N′) Higher magnification images of the regions boxed in (M) and (N).

(O and P) Reduced Alcian blue staining in *Nfatc1*[Cre]; *Pdcd10*^{fl/fl} hearts at E12.5.

(Q and R) Reduced intact versican in in *Nfatc1*[Cre]; *Pdcd10*^{fl/fl} hearts at E12.5. Scale bars represent 100 μm.

myocardial growth and trabeculation (Grego-Bessa et al., 2007; Somekawa et al., 2012), were also detected (Figures 3A and 3C). Expression of the myocardial growth factors FGF9, FGF12 and FGF16 (Lavine et al., 2005) was unaltered, while that of neuregulin was elevated in E10.5 *Nfatc1*[Cre];*Krit1*^{fl/fl} hearts (Figure 3C), indicating that reduced myocardial growth did not result from reduced endocardial expression of growth factors. The expression of *Versican* and *HA synthase* were also unchanged, despite the dramatic loss of versican protein detected in *Nfatc1*[Cre];*Krit1*^{fl/fl} hearts (Figure 3D). In situ hybridization confirmed the increase in *Klf2* mRNA in the E10.5 *Nfatc1*[Cre];*Krit1*^{fl/fl} heart (Figure 3E). KLF4 protein was not detected in the endocardium of the heart chamber in control animals at E10.5, but was present in the nuclei of almost all the endocardial cells in the E10.5 *Nfatc1*[Cre]; *Krit1*^{fl/fl} heart (Figure 3F). Increased levels of KLF2 protein were also detected by western blot analysis of the E10.5 *Nfatc1*[Cre]; *Krit1*^{fl/fl} heart (Figure 3G). Significantly, similar changes in *Klf* and *Adamts* gene expression were observed in the E11.5 *Nfatc1*[Cre];*Pdcd10*^{fl/fl} heart (Figure S2), consistent with a requirement for canonical CCM signaling in the regulation of these genes.

The gene expression studies described above suggested that excess ADAMTS4/5 activity might be the cause of reduced

expression of myocardial growth factors and components of the cardiac jelly such as hyluronic acid. Alternatively, endocardial CCM signaling might be required to prevent the expression of proteases such as those in the ADAMTS family that cleave versican and degrade cardiac jelly at later time points during cardiac development (Stankunas et al., 2008; Dupuis et al., 2011). To address these possible mechanisms we characterized gene expression in whole E10.5 *Nfatc1*[Cre];*Krit1*^{fl/fl} and littermate control hearts using microarray and qPCR analysis. Microarray and qPCR analysis revealed elevated levels of *Adamts4* and *Adamts5*, versican-degrading proteases, in addition to *Klf2* and *Klf4* and a number of known KLF2/4 target genes, including *Nos3, Aqp1, Jam2, Thbd,* and *Palmd* (Dekker et al., 2006; Parmar et al., 2006) (Figures 3A, 3B, and 3D). Reduced levels of *Dll4* and *Tmem100*, genes previously associated with
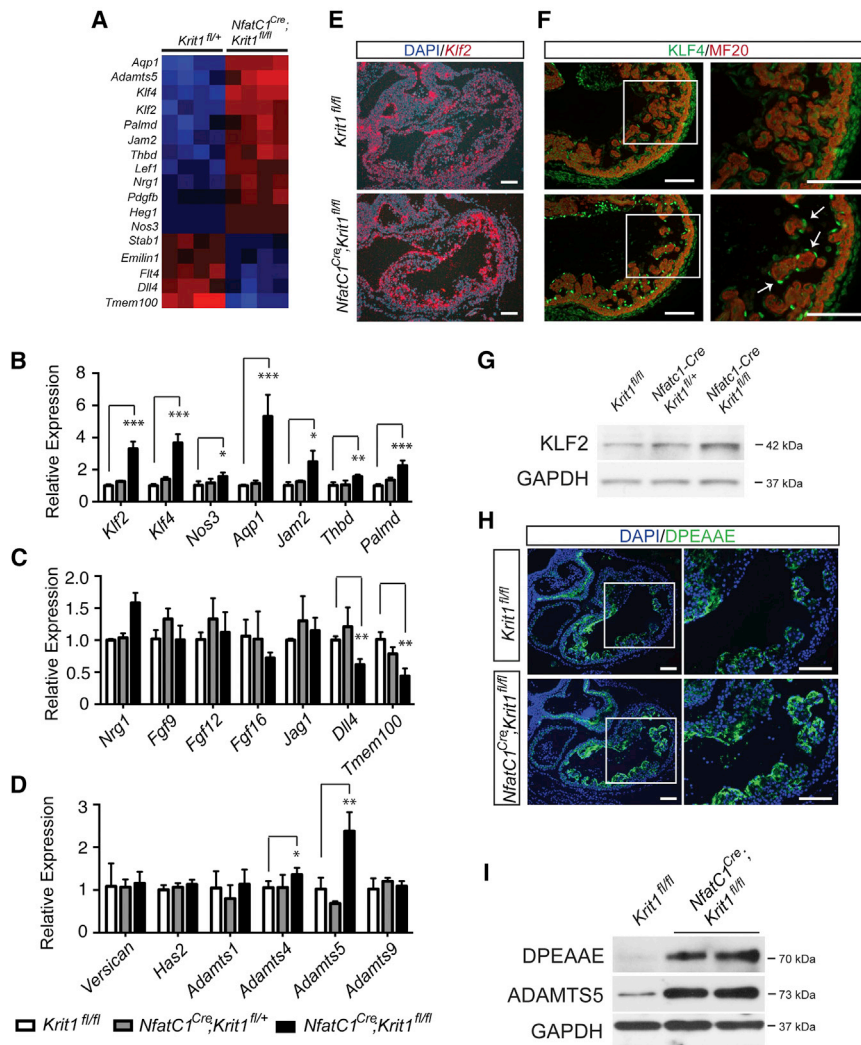
Figure 3. Loss of CCM Signaling Results in Increased *Klf2* and *Adamts5* Expression and Function

(A) Microarray analysis of mRNA expression in E10.5 *Nfatc1*^{Cre};*Krit1*$^{fl/fl}$ and *Krit1*$^{fl/+}$ littermate hearts reveals increased levels of *Klf2*, *Klf4*, KLF2 target genes and *Adamts5*, and reduced levels of *Dll4* and *Tmem100*. N = 4 for both genotypes.

(B) qPCR of E10.5 hearts reveals preserved or increased expression of *Nrg1* and FGF growth factors following endocardial *Krit1* loss.

(C) qPCR of E10.5 hearts reveals elevated levels of *Klf2* and established KLF2 target genes following endocardial *Krit1* loss.

(D) qPCR analysis of genes associated with cardiac jelly matrix proteins and matrix-degrading proteases in E10.5 hearts reveals elevated levels of *Adamts5* following endocardial *Krit1* loss. N = 3 for *Krit1*$^{fl/fl}$, N = 4 for *Nfatc1*^{Cre};*Krit1*$^{fl/+}$, N = 5 for *Nfatc1*^{Cre};*Krit1*$^{fl/fl}$ in (B)–(D).

(E) In situ hybridization for *Klf2* in E10.5 *Nfatc1*^{Cre};*Krit1*$^{fl/fl}$ and *Krit1*$^{fl/fl}$ littermate hearts.

(F) Immunostaining for KLF4 protein (arrows) and myocardium (MF20) in E10.5 *Nfatc1*^{Cre};*Krit1*$^{fl/fl}$ and *Krit1*$^{fl/fl}$ littermate hearts.

(G) Immunoblot analysis of KLF2 protein in whole E10.5 *Nfatc1*^{Cre};*Krit1*$^{fl/fl}$ and *Nfatc1*^{Cre};*Krit1*$^{fl/+}$ and *Krit1*$^{fl/fl}$ littermate hearts. GAPDH is shown as a loading control.

(H) Immunostaining using anti-DPEAAE antibody to detect ADAMTS-cleaved versican reveals increased levels in the E10.5 *Nfatc1*^{Cre};*Krit1*$^{fl/fl}$ heart. Boxed regions are shown at higher magnification on the right.

(I) Immunoblot analysis of lysate derived from whole E10.5 hearts reveals increased levels of cleaved versican (DPEAAE) and the ADAMTS5 protease with endocardial loss of *Krit1*. GAPDH is shown as a loading control. Scale bars represent 100 μm. *p < 0.05; **p < 0.01; ***p < 0.001.

versican and cardiac jelly in *Nfatc1*^{Cre};*Krit1*$^{fl/fl}$ hearts. To detect ADAMTS-mediated breakdown of versican, we stained *Nfatc1*^{Cre};*Krit1*$^{fl/fl}$ and control E10.5 hearts with antibodies that specifically recognize a versican epitope that is exposed following cleavage by ADAMTS proteases ("DPEAAE" antibody) (Sandy et al., 2001). Despite the nearly complete loss of intact versican (Figures 1H and 1I), increased levels of ADAMTS-cleaved versican were detected in the E10.5 *Nfatc1*^{Cre};*Krit1*$^{fl/fl}$ heart by immunostaining with DPEAAE antibody (Figure 3H). Biochemical analysis of whole E10.5 *Nfatc1*^{Cre};*Krit1*$^{fl/fl}$ hearts confirmed a marked increase in the levels of cleaved versican and ADAMTS5 protease (Figure 3I). These findings tie the loss of cardiac jelly associated with endocardial loss of CCM signaling to changes in endocardial gene expression.

Loss of *klf2* or *adamts5* Rescues Loss of CCM Signaling in Zebrafish Embryos

Endocardial-specific loss of CCM signaling in the mouse results in a thin, dilated heart that lacks cardiac jelly/matrix (Figures 1 and 2). This phenotype resembles the dilated heart in zebrafish embryos lacking this pathway (Mably et al., 2003, 2006), sug-

gestive of a conserved role for CCM signaling in vertebrate cardiac development. To determine if loss of CCM signaling results in loss of cardiac jelly/matrix in developing fish as well as mice we analyzed sections of 72 high-power field (hpf) *ccm2* mutant and control littermate hearts using H&E and Alcian blue staining. Control hearts exhibited a multicellular layer of myocardium, with detectable Alcian blue-stained cardiac jelly between the endocardial and myocardial cell layers (Figures 4A–4C). In contrast, *ccm2* mutant hearts exhibited a thin, single-cell layer of myocardium, and no Alcian blue staining was detected in sections that sampled the entire heart (Figures 4D–4F, N = 4 embryos studied for each genotype). Thus, CCM signaling deficiency results in the loss of cardiac jelly in both fish and mouse embryos, consistent with a conserved role for this pathway during heart development.

Molecular analysis of E10.5 *Nfatc1*^{Cre};*Krit1*$^{fl/fl}$ and E10.5 *Nfatc1*^{Cre};*Pdcd10*$^{fl/fl}$ mouse hearts revealed significant upregulation of *Klf2/4* and *Adamts4/5* gene expression, suggesting that these genes might play causal roles in the cardiac phenotype. To functionally test a conserved role for regulation of KLF2 and ADAMTS5 by CCM signaling, we next studied 72 hpf
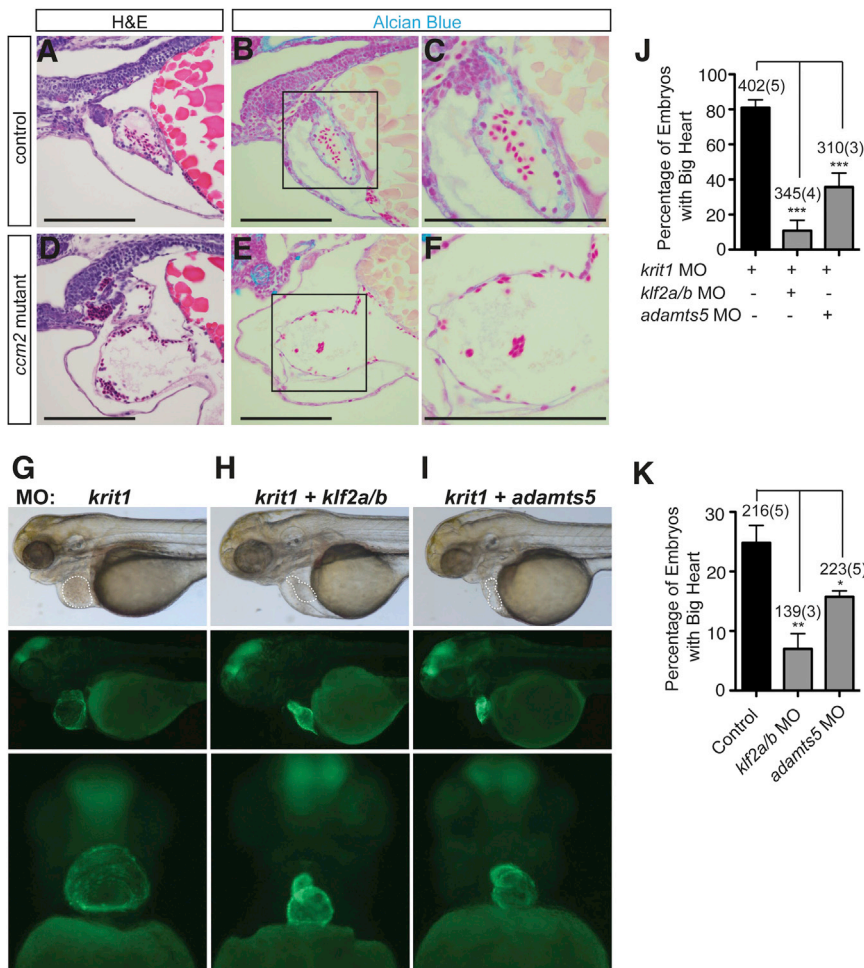
Figure 4. Loss of *klf2* or *adamts5* Rescues the Cardiac Phenotype Conferred by Loss of CCM Signaling in Zebrafish Embryos

(A–C) H&E and Alcian blue staining of adjacent sections from a 72 hpf control zebrafish heart reveal a myocardial wall with multiple cell layers (A) and the presence of Alcian blue-staining cardiac jelly (B and C).

(D–F) H&E and Alcian blue staining of adjacent sections from a 72 hpf *ccm2* mutant heart reveals a thin myocardial wall (D) and lack of cardiac jelly (E and F). (C and F) Higher magnification images of the boxed regions in (B) and (E).

(G) Injection of zebrafish embryos with *krit1* morpholinos results in a big heart at 72 hpf detected by light microscopy and in *i-fabp*:GFP transgenic embryos in which the heart is fluorescently labeled.

(H) Injection of morpholinos targeting both *krit1* and the two *klf2* zebrafish orthologs rescues the big heart phenotype at 72 hpf.

(I) Injection of morpholinos targeting both *krit1* and *adamts5* rescues the big heart phenotype at 72 hpf.

(J) Efficiency of rescue of the *krit1* morphant heart phenotype with *klf2* and *adamts5* morpholinos. ***p < 0.001.

(K) Knockdown of *klf2* or *adamts5* also rescues the cardiac phenotype in *ccm2* mutant zebrafish embryos. The frequency of a big heart phenotype in the offspring of *ccm2*$^{+/-}$ intercrosses treated with control, *klf2* or *adamts5* morpholinos is shown. **p < 0.01; *p < 0.05. The number of total embryos analyzed and number experimental repeats (in parentheses) in (J) and (K) are indicated above each bar. Scale bars represent 100 μm.

zebrafish embryos following injection of morpholinos to block expression of *krit1*, with or without co-injection of morpholinos to block *klf2*a and *klf2*b (the two zebrafish *Klf2* orthologs) or *adamts5* (the sole zebrafish *Adamts5* ortholog). *krit1* morpholinos resulted in a dilated heart in approximately 80% of embryos at 72 hpf (Figures 4G and 4J). When combined with low dose *klf2*a/b morpholinos (1.5 ng each) that resulted in a reduction of approximately 50% in *klf2* dosage (Figure S3), we observed highly efficient rescue of the big heart phenotype (approximately 90% rescue efficiency, p < 0.001) (Figures 4H and 4J). Co-injection of morpholinos targeting the exon 2 splice acceptor and donor sites of *adamts5* (5+1 ng, a combination chosen to minimize morpholino dose and toxicity, Figures S4C and S4D) also resulted in a significant rescue of the big heart phenotype (approximately 50% rescue efficiency, p < 0.001) (Figures 4I and 4J). To ensure that rescue was not merely due to interference with *krit1* morpholinos, *klf2* or *adamts5* morpholinos were injected into embryos generated by *ccm2*$^{+/-}$ intercrosses. As expected, a big heart phenotype was observed in approximately 25% of control offspring at 72 hpf (Figure 4K). However, this cardiac phenotype was observed in only 7% and 16% of offspring injected with *klf2*a/b or *adamts5* morpholinos, respectively (indicative of a 70% and 35% rescue efficiency for *klf2* and *adamts5*, respectively; p < 0.01 and p < 0.05) (Figure 4K). The

lower efficiency of mutant rescue compared with morphant rescue most likely reflects the greater loss of CCM signaling in *ccm2*$^{-/-}$ mutants compared with *krit1* morphants. These studies suggest that a critical and conserved role of CCM signaling in the developing heart is to negatively regulate the expression of *Klf2* and *Adamts5*.

MEKK3 Regulates *KLF* and *ADAMTS* Gene Expression in Cultured Endothelial Cells and in Embryonic Endocardium

The findings described above revealed that CCM signaling negatively regulates *Klf2* and *Adamts5* gene expression, but studies of signaling by the CCM adaptor proteins have not defined a transcriptional mechanism of action. How are these pathways linked? MEKK3 was identified as a CCM2 binding partner a decade ago (Uhlik et al., 2003), and MEKK3 signaling is known to regulate gene expression through downstream effectors such as ERK5 and MEF2C (Chao et al., 1999; Nakamura and Johnson, 2003), as well as p38 and JNK (Deacon and Blank, 1999; Nebreda and Porras, 2000). We therefore next explored the possibility that CCM signaling might alter expression of KLF2 and ADAMTS5 through effects on the MEKK3 pathway. Because available anti-CCM2 antibodies are unable to detect the protein in cultured endothelial cells, to determine if MEKK3
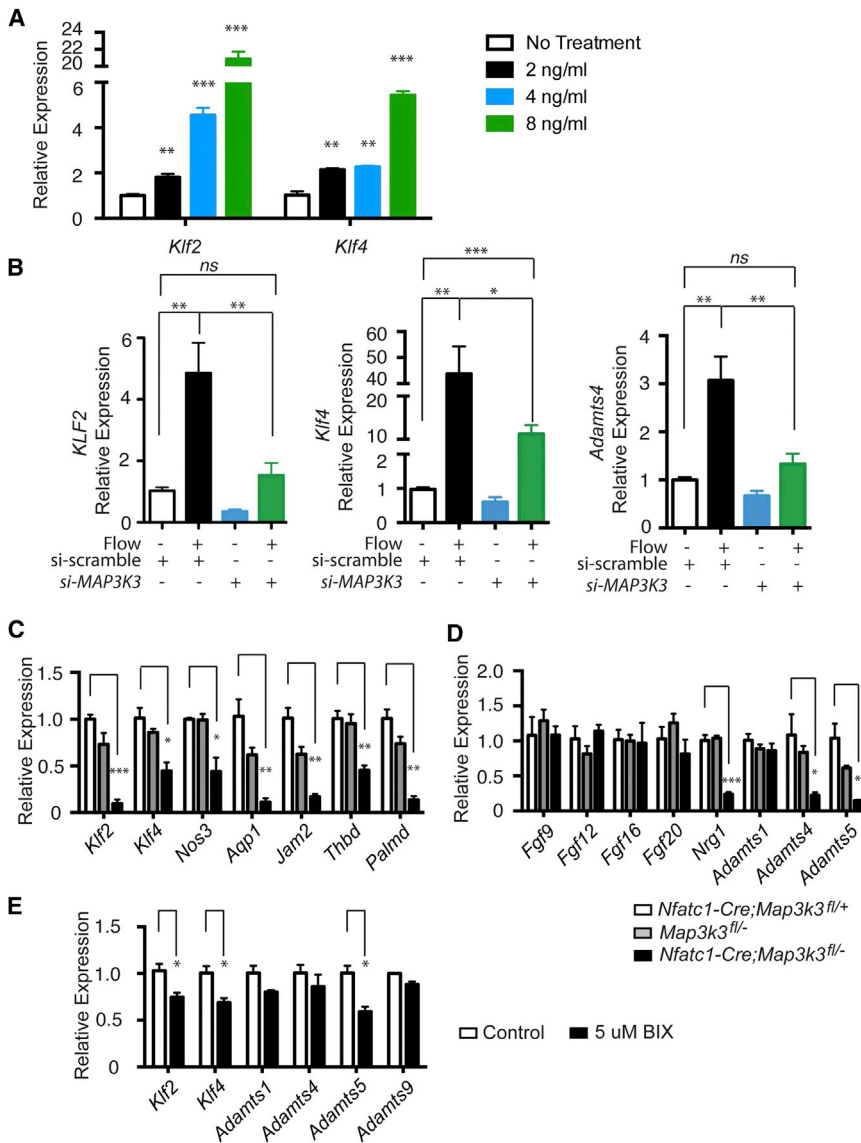
Figure 5. MEKK3 Regulates Expression of *KLF* and *ADAMTS* Genes in Cultured Endothelial Cells and in the Endocardium of the Developing Heart

(A) Tetracycline-regulated expression of BirA-MEKK3 drives dose-dependent expression of *KLF2* and *KLF4* in HUVEC.

(B) siRNA knockdown of *MEKK3* in HUVEC blocks flow-induced expression of *KLF2, KLF4* and *ADAMTS4*. HUVEC were exposed to 16 hr of laminar shear after exposure to siRNA directed against *MEKK3 (MAP3K3)* or control, scrambled siRNA. N = 5; p < 0.0001.

(C) qPCR of E10.5 hearts reveals severely reduced levels of *Klf2, Klf4* and known KLF2/4 target genes following endocardial *Mekk3 (Map3k3)* deletion. N = 3 for all groups.

(D) qPCR of E10.5 hearts reveals reduced levels of *Nrg1* and *Adamts5* but normal levels of FGFs following endocardial *Mekk3 (Map3k3)* deletion. N = 3 for all groups.

(E) qPCR of E9.5 wild-type mouse hearts following 24 hr incubation in medium containing the MEK5 inhibitor BIX02188 ("BIX") or DMSO ("control"). N = 3 for all groups. Error bars represent SEM. *p < 0.05; **p < 0.01; ***p < 0.001; ****p < 0.0001.

interacts with CCM proteins in endothelial cells we used tetracycline-regulable lentiviral vectors to express an BirA-MEKK3 fusion protein in hCMEC/D3 endothelial cells (Weksler et al., 2005) (Figure S4). Using this approach, MEKK3-interacting proteins were biotinylated in live endothelial cells (Roux et al., 2012). Biotinylated proteins were captured by streptavidin beads and subjected to mass spectrometry analysis. When BirA-MEKK3 was expressed at endogenous levels (4 ng/ml doxycycline, Figure S4A), no specific MEKK3-interacting proteins were identified (not shown), perhaps due to kinase inactivity. At slightly higher expression levels (8 ng/ml doxycycline) peptides from only four interacting proteins were identified (Figure S4). The most abundant of these was CCM2 (Figure S4E). KRIT1 was also detected at a lower level equivalent to that of TRAF7, an MEKK3-interacting protein previously identified using tandem affinity purification (Bouwmeester et al., 2004). A similar result was obtained when BirA-MEKK3 was expressed in primary human umbilical vein endothelial cells (HUVECs; Figure S4F). These studies indicate

that MEKK3 interacts with the CCM protein complex in live endothelial cells.

To determine if MEKK3 regulates endothelial gene expression in a manner that might explain the changes observed following loss of CCM signaling, we next tested whether MEKK3 is sufficient and/or required for *KLF* and *ADAMTS* gene expression in cultured endothelial cells. Overexpression of MEKK3 using the doxycycline regulable system described above resulted in dose-dependent increases in the levels of *KLF2* and *KLF4* expression in hCMEC/D3 endothelial cells (Figure 5A). To determine whether MEKK3 regulates *KLF* gene expression in response to more physiologic stimuli, we tested the role of MEKK3 in endothelial responses to fluid flow. Flow and fluid shear forces are established regulators of *KLF2* and *KLF4* expression in endothelial cells ex vivo (Huddleson et al., 2004; Parmar et al., 2006; Sohn et al., 2005; Villarreal et al., 2010) and in humans (Dekker et al., 2006), mice (Dekker et al., 2006; Lee et al., 2006), chick (Groenendijk et al., 2005), and fish (Vermot et al., 2009) in vivo. Upregulation of *KLF2* in response to flow has been shown to be mediated by MEK5-ERK5 signaling (Li et al., 2008; Parmar et al., 2006), one of the pathways directly regulated by MEKK3(Chao et al., 1999; Nakamura and Johnson, 2003). Consistent with prior studies (Parmar et al., 2006; Sohn et al., 2005), HUVECs exposed to laminar shear for 16 hr exhibited increased *KLF2, KLF4* and *ADAMTS4* expression (Figure 5B). Transfection with siRNAs directed against *MEKK3* that resulted in a 40% knockdown in *MEKK3* expression blocked the rise in expression of *KLF2, KLF4*, and *ADAMTS4* induced by flow (Figure 5B). These studies
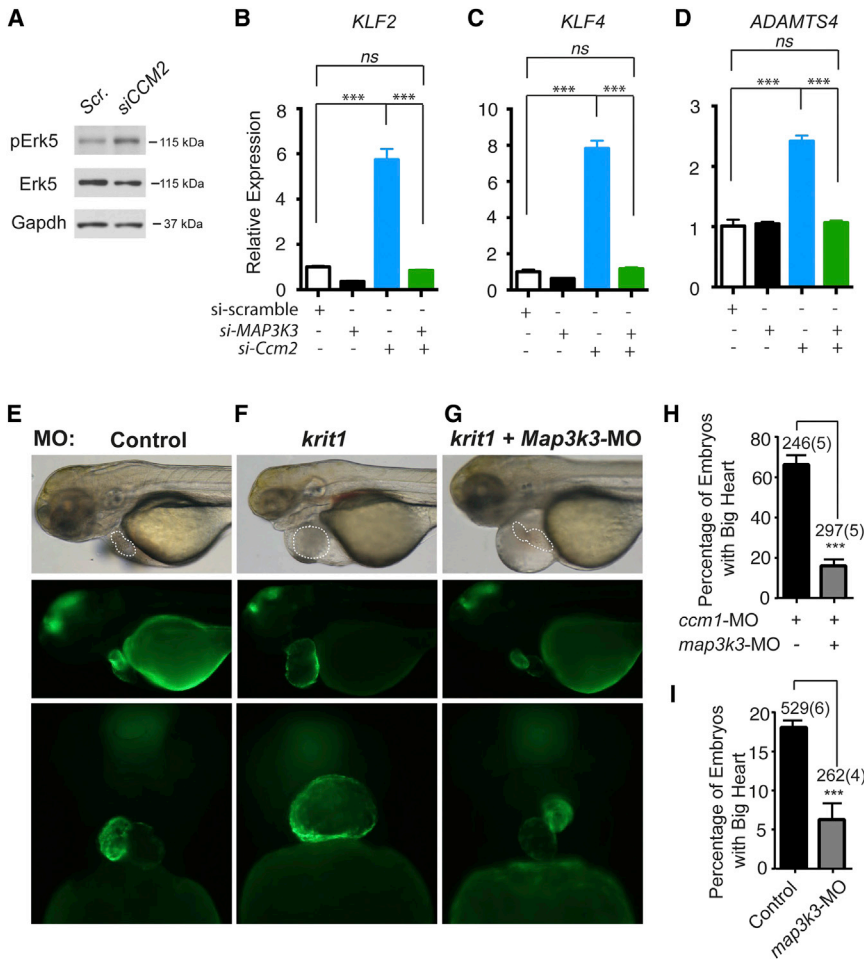
Figure 6. Loss of MEKK3 Rescues the CCM-Deficient Phenotype in Cultured Endothelial Cells and Zebrafish Embryos

(A) siRNA knockdown of CCM2 increases the level of phospho-ERK5 in cultured HUVEC.

(B–D) siRNA knockdown of CCM2 increases the expression of KLF2, KLF4, and ADAMTS4 in HUVEC, and these changes in gene expression are reversed by siRNA knockdown of MEKK3 (MAP3K3). Error bars represent SEM.

(E and F) Injection of zebrafish embryos with krit1 morpholinos results in a big heart at 72 hpf in i-fabp:GFP transgenic embryos in which the heart is fluorescently labeled.

(G) Injection of morpholinos targeting both krit1 and map3k3 rescues the big heart phenotype at 72 hpf.

(H) Efficiency of rescue of the krit1 morphant heart phenotype with map3k3 morpholinos. ***p < 0.001.

(I) Knockdown of map3k3 rescues the cardiac phenotype in ccm2 mutant zebrafish embryos. The frequency of a big heart phenotype in the offspring of ccm2+/− intercrosses treated with control or map3k3 morpholinos is shown. ***p < 0.001. The number of total embryos analyzed and number experimental repeats (in parentheses) are indicated above each bar in (H) and (I); Error bars represent SEM. Scale bars represent 100 μm.

et al., 2008). Treatment with BIX02189 resulted in reduced levels of *Klf2, Klf4,* and *Adamts5* expression (Figure 5E). These findings demonstrate that MEKK3 regulates *KLF* and *ADAMTS* gene expression in endothelial cells ex vivo and in endocardial cells in vivo through the MEK5-ERK5 MAPK pathway.

Loss of MEKK3 Rescues Loss of CCM Signaling in Cultured Endothelial Cells and Zebrafish Embryo Hearts

The reciprocal changes in gene expression observed with endocardial loss of CCM and MEKK3 signaling, the physical interaction between the CCM complex and MEKK3, and the preservation of *Mekk3* gene expression in *Nfatc1^Cre;Krit1^fl/fl* hearts (Figure S6A) suggested that CCM signaling might regulate endocardial gene expression by inhibiting MEKK3 function. To test the effect of loss of CCM signaling on MEKK3 function, we used siRNA to knockdown *CCM2* in HUVECs and examined downstream MEKK3 signaling through ERK5. HUVECs treated with *CCM2* siRNA, but not with scrambled siRNA, exhibited increased phospho-ERK5 with no change in total ERK5 or GAPDH protein (Figure 6A), consistent with an increase in MEKK3 pathway activity. As observed with endocardial deletion in the E10.5 mouse heart, loss of *CCM2* in HUVEC conferred increased expression of *KLF2*, *KLF4*, and *ADAMTS4* (Figures 6B–6D). These increases were reversed by simultaneous knockdown of *MEKK3*, consistent with CCM regulation of gene expression through MEKK3.

To test whether increased MEKK3 signaling is causal for CCM-deficient phenotypes in vivo, we first used morpholinos

reveal that *KLF* and *ADAMTS* expression are regulated by MEKK3 in cultured endothelial cells.

To determine whether MEKK3 also regulates these genes in the E10.5 heart, we next generated *Nfatc1^Cre;Map3k3^fl/−* animals. *Nfatc1^Cre;Map3k3^fl/−* animals did not survive to birth, and timed matings revealed embryonic lethality prior to E12.5 (Table S1). Analysis of *Nfatc1^Cre;Map3k3^fl/−* embryonic heart sections revealed a thin myocardial cell layer with preserved cardiac jelly and normal endocardial-myocardial separation at E10.5 (Figure S5A). In contrast to endocardial loss of CCM signaling, versican levels were preserved in the E10.5 *Nfatc1^Cre; Map3k3^fl/−* heart (Figure S5B). Gene expression analysis of E10.5 *Nfatc1^Cre;Map3k3^fl/−* and control littermate hearts revealed severe (>90%) reductions in the expression of *Klf2* and the known KLF2 target genes *Nos3, Aqp1, Jam2, Thbd,* and *Palmd*, as well as *Klf4, Adamts4,* and *Adamts5* (Figures 5C and 5D). FGF gene expression was unchanged but the expression of *Nrg1* was severely reduced (Figure 5D). Thus, loss of MEKK3 confers gene expression changes that are precisely reciprocal to those conferred by loss of KRIT1 or PDCD10. To determine whether MEKK3 regulates *Klf* and *Adamts* gene expression through the ERK5 MAPK pathway, we cultured wild-type E10.5 explanted hearts in the presence of BIX02189, a highly specific inhibitor of MEK5, the MAPK2K that is activated by MEKK3 and in turn activates ERK5 (Tatake

to reduce the levels of *mekk3* in *krit1* morphant and *ccm2* mutant zebrafish embryos. *krit1* morpholinos resulted in a dilated heart in approximately 65% of embryos at 72 hpf in these studies (Figures 6E, 6F, and 6H). When combined with low-dose morpholinos (3 ng) that resulted in a reduction of approximately 40% in *mekk3* dosage (Figure S7) but had no independent effect on cardiac development, we observed efficient (~75%) rescue of the *krit1* morphant cardiac phenotype (p < 0.001) (Figures 6G and 6H). To ensure that rescue was not due to interference with *krit1* morpholinos, *mekk3* morpholinos were injected into embryos generated by *ccm2*$^{+/-}$ intercrosses. A big heart phenotype was observed in approximately 18% of control morpholino injected offspring at 72 hpf, and injection of low-dose *mekk3* morpholinos reduced this to approximately 6%, consistent with a 66% rescue efficiency (p < 0.001, Figure 6I). Thus, loss of *mekk3* rescues the dilated heart phenotype conferred by loss of either *krit1* or *ccm2* in zebrafish embryos, suggesting that gain of MEKK3 signaling may underlie the role of CCM signaling during cardiac development.

Mekk3 Haplo-Insufficiency Rescues the Loss of Cardiac Jelly and Changes in Gene Expression Conferred by Endocardial *Krit1* Deletion

Rescue of the big heart phenotype conferred by loss of CCM signaling with loss of *mekk3* expression in the zebrafish requires careful dosing of *mekk3* morpholinos to avoid an independent mekk3-deficient cardiac defect, and the ability to measure rescue using specific molecular and cellular endpoints is limited in the zebrafish embryo heart. To address these issues and rigorously test the causal role of the MEKK3 pathway as a downstream CCM effector in mammals, we next tested the ability of loss of one *Mekk3* allele to rescue the specific changes in cardiac jelly and cardiac gene expression in the E10.5 *Nfatc1*^{Cre};*Krit1*$^{fl/fl}$ mouse heart. Despite the expected loss in MEKK3 protein in *Map3k3*$^{+/-}$ hearts (Figure S6C), *Map3k3*$^{+/-}$ animals and *Nfatc1*^{Cre};*Map3k3*$^{fl/+}$ animals develop normally, exhibit no changes in cardiac jelly, and have patterns of cardiac gene expression at E10.5 that are indistinguishable from *Map3k3*$^{fl/fl}$ littermates (Yang et al., 2000 and data not shown). Thus, loss of a single *Mekk3* allele is well tolerated and does not affect cardiac development. At E10.5, *Nfatc1*^{Cre};*Krit1*$^{fl/fl}$;*Map3k3*$^{fl/+}$ hearts exhibited significantly more cardiac jelly, Alcian blue staining, and intact versican than was seen in *Nfatc1*^{Cre};*Krit1*$^{fl/fl}$;*Map3k3*$^{+/+}$ littermates (Figures 7A–7I). Quantitation of the area occupied by cardiac jelly in the trabeculae of E10.5 littermate hearts revealed a >65% decrease in *Nfatc1*^{Cre};*Krit1*$^{fl/fl}$ hearts compared with control littermates, but only a 25% decrease in *Nfatc1*^{Cre};*Krit1*$^{fl/fl}$;*Map3k3*$^{fl/+}$ hearts (p < 0.001, Figure 7J). Consistent with the rescue of cardiac jelly, biochemical analysis of ADAMTS-proteolyzed versican using anti-DPEAAE antibodies revealed increased versican breakdown in the *Nfatc1*^{Cre};*Krit1*$^{fl/fl}$ heart that was restored to normal levels in the *Nfatc1*^{Cre};*Krit1*$^{fl/fl}$;*Map3k3*$^{fl/+}$ heart (Figure 7K). qPCR analysis of cardiac gene expression revealed significantly reduced levels of *Klf2*, *Klf4*, KLF2/4 target genes, *Adamts4* and *Adamts5*, and *Nrg1*, and increased levels of *Dll4* and *Tmem100*, in the *Nfatc1*^{Cre};*Krit1*$^{fl/fl}$;*Map3k3*$^{fl/+}$ heart compared with the *Nfatc1*^{Cre};*Krit1*$^{fl/fl}$;*Map3k3*$^{+/+}$ heart (Figures 7L–7N). The levels of *Klf2, Klf4* and *Adamts5* gene expression were not restored to normal in the *Nfatc1*^{Cre};*Krit1*$^{fl/fl}$;*Map3k3*$^{fl/+}$

heart, consistent with the significant but incomplete histologic rescue. Thus virtually all of the hallmark histologic, biochemical, and genetic changes observed with endocardial loss of KRIT1 are rescued by endocardial loss of MEKK3, indicating that gain of MEKK3 signaling plays a central, causal role in the endothelial phenotype conferred by loss of CCM signaling in the developing heart.

DISCUSSION

Genetic studies in humans, mice, and fish have revealed that CCM signaling is required in endothelial cells for normal cardiovascular development and to prevent vascular malformations after birth, but the molecular basis for these phenotypes has remained elusive. We have used studies of cultured endothelial cells, endocardial-specific deletion in the developing mouse, and genetic rescue of the CCM-deficient heart phenotype in both mice and zebrafish to reveal a molecular mechanism by which the CCM pathway regulates endothelial gene expression. Our studies demonstrate that CCM signaling in the endocardium plays a critical and conserved role in cardiac development through regulation of the MEKK3 MAPK signaling pathway and downstream ADAMTS and KLF gene expression.

A role for CCM signaling in cardiac development was revealed by the dilated heart phenotype observed in zebrafish embryos lacking this pathway (Mably et al., 2003, 2006; Zheng et al., 2010), but the molecular and cellular basis for this phenotype has been unclear. The studies reported here demonstrate that CCM signaling controls degradation of cardiac jelly by negatively regulating endocardial expression of ADAMTS4/5 and KLF2/4. A causal role for excess ADAMTS4/5 is demonstrated by a dramatic increase in versican cleavage associated with loss of cardiac jelly in the *Nfatc1*^{Cre};*Krit1*$^{fl/fl}$ mouse heart and by rescue of the zebrafish dilated heart with morpholinos that reduced *adamts5* levels. Expression of both *Adamts* and *Klf* genes is severely reduced following endothelial loss of MEKK3 in vitro and in vivo, increased MEKK3 drives expression of both genes in cultured endothelial cells, rescue of *krit1* morphant and *ccm2* mutant zebrafish hearts was highly efficient with loss of *mekk3*, *klf2*, or *adamts5*, and both the histologic and molecular phenotypes conferred by loss of endocardial CCM signaling are rescued by partial loss of MEKK3. Thus a straightforward pathway is one in which changes in MEKK3 signaling alter expression of KLF2/4 that in turn controls expression of ADAMTS4/5 (Figure 7O). However, *Adamts5* has not been identified as a KLF2 target gene in cultured endothelial cells (Dekker et al., 2002; Parmar et al., 2005), and we do not detect *Adamts5* expression in HUVEC. Thus, *Adamts4/5* may be regulated by MEKK3 in a KLF-independent manner, or by KLF2/4 in embryonic endocardium but not in cultured endothelial cells. It is also likely that MEKK3-regulated and KLF-regulated genes other than *Adamts4/5* contribute to the cardiac phenotype associated with CCM deficiency. Two such candidates identified by our gene expression studies are *Dll4*, a Notch ligand expressed by the endocardium that supports trabeculation and myocardial proliferation (Grego-Bessa et al., 2007), and *Tmem100*, an ALK1 target gene that is also specifically expressed in the endocardium and required for cardiac growth (Somekawa et al., 2012). In this regard, it is intriguing that KLF4 has recently been
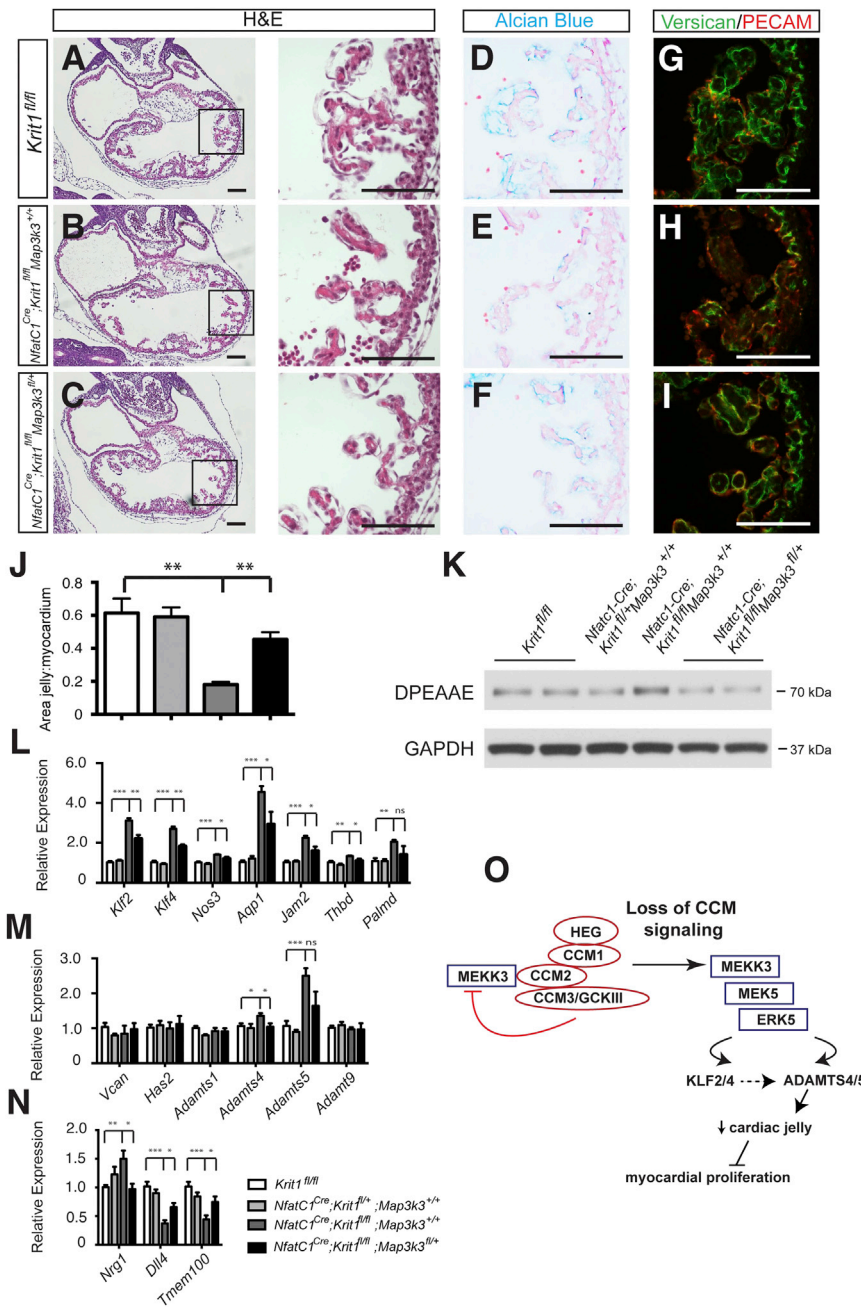
Figure 7. Reduced *Mekk3* Expression Rescues the Loss of Cardiac Jelly and Changes in Gene Expression Conferred by Endocardial Loss of *Krit1*

(A–C) The endocardial-myocardial space occupied by cardiac jelly is increased in *Nfatc1^Cre*;*Krit1^fl/fl*;*Map3k3^fl/+* hearts compared with *Nfatc1^Cre*;*Krit1^fl/fl*;*Map3k3^+/+* littermates at E10.5. Higher magnification images of the boxed regions are shown on the right.

(D–F) Alcian blue staining for cardiac jelly is increased in *Nfatc1^Cre*;*Krit1^fl/fl*;*Map3k3^fl/+* hearts compared with *Nfatc1^Cre*;*Krit1^fl/fl*;*Map3k3^+/+* littermates at E10.5.

(G–I) Versican in cardiac jelly is increased in *Nfatc1^Cre*;*Krit1^fl/fl*;*Map3k3^fl/+* hearts compared with *Nfatc1^Cre*;*Krit1^fl/fl*;*Map3k3^+/+* littermates at E10.5.

(J) The ratio of the area occupied by cardiac jelly to that occupied by myocardium in the trabeculae is increased in E10.5 *Nfatc1^Cre*;*Krit1^fl/fl*;*Map3k3^fl/+* hearts compared with *Nfatc1^Cre*;*Krit1^fl/fl*;*Map3k3^+/+* littermates. N = 3 embryos; nine sections analyzed for each group. Error bars indicate SEM.

(K) Immunoblot analysis of lysate derived from whole E10.5 hearts reveals higher levels of cleaved versican (DPEAAE) in *Nfatc1^Cre*;*Krit1^fl/fl*;*Map3k3^+/+* hearts compared with *Nfatc1^Cre*;*Krit1^fl/fl*;*Map3k3^fl/+* littermates. GAPDH is shown as a loading control.

(L–N) qPCR of E10.5 hearts reveals normalized expression of *Klf2*, *Klf4*, KLF2/4 target genes, *Nrg1*, *Dll4*, *Tmem100*, *Adamts4* and *Adamts5* in *Nfatc1^Cre*;*Krit1^fl/fl*;*Map3k3^fl/+* hearts compared with *Nfatc1^Cre*;*Krit1^fl/fl*;*Map3k3^+/+* littermates at E10.5. *p < 0.05; **p < 0.01; ***p < 0.001. Scale bars represent 100 μm. Error bars indicate SEM.

(O) CCM regulation of MEKK3 activity and gene expression. The CCM complex binds MEKK3 through interaction with CCM2 and blocks MEKK3 signaling (left). Loss of the CCM complex increases MEKK3-ERK5 signaling and the expression of *Klf2* and *Adamts5*, resulting in the breakdown of cardiac jelly and reduced myocardial proliferation (right).

MEKK3 signaling (Figure 7O). Rescue of CCM-deficient phenotypes in cultured endothelial cells and fish and mouse embryos demonstrates a clear causal role for increased MEKK3 function. Previous studies have linked MEKK3 to three downstream MAPK pathways by which it might regulate gene expression: JNK (Deacon and Blank, 1999), p38 (Deacon and Blank, 1999; Uhlik et al., 2003), and ERK5 (Chao et al., 1999; Nakamura and Johnson, 2003). However, our endothelial studies demonstrate MEKK3 regulation of KLF2/4 and ADAMTS4 expression in response to fluid flow, known to be downstream of MEK5 and ERK5 (Li et al., 2008; Parmar et al., 2006; Sohn et al., 2005), and ex vivo embryonic heart culture studies using a highly specific MEK5 inhibitor identify the MEK5-ERK5 pathway as a key mechanism of gene regulation by CCM signaling (Figure 5). Thus, our studies support a mechanism in which CCM signaling

shown to repress *DLL4* expression in endothelial cells (Hale et al., 2014).

A key finding to emerge from our studies is the identification of a molecular mechanism by which CCM signaling regulates endothelial gene expression. Previous studies of the CCM pathway have not revealed a molecular path to transcriptional regulation, although changes in RhoA activity (Glading et al., 2007; Stockton et al., 2010; Whitehead et al., 2009; Zheng et al., 2010) and TGFb signaling (Maddaluno et al., 2013) have been reported. The findings that CCM2 interacts with MEKK3 in endothelial cells and that endocardial loss of CCM signaling and MEKK3 confer precisely reciprocal changes in gene expression suggested that the CCM pathway may control gene expression by regulating

specifically regulates the MEK5-ERK5 pathway downstream of MEKK3 in endothelial cells.

A final question raised by our studies is whether regulation of the MEKK3 pathway by CCM signaling observed in the developing heart also plays an important role in the formation of CCMs in humans and mice. Loss of CCM signaling in the postnatal endothelium results in large vascular malformations (CCMs) in the CNS of humans and mice (Akers et al., 2009; Boulday et al., 2011; Chan et al., 2011; McDonald et al., 2011). CCMs are an important cause of stroke for which there is presently no medical treatment (Li and Whitehead, 2010). Drugs that inhibit RhoA and TGFb signaling have been reported to reduce lesion frequency in mouse models of CCM (Maddaluno et al., 2013; McDonald et al., 2012), but the responses have been incomplete and a clear molecular and/or cellular basis for CCM formation is still lacking. Significantly, upregulation of KLF4 expression was recently identified as a prominent molecular phenotype of the endothelial cells that form CCMs (Maddaluno et al., 2013), a finding that mirrors the increase in KLF4 observed in the developing endocardium and in cultured endothelial cells lacking CCM signaling. It is therefore possible that CCM-deficient endothelial cells in the CNS exhibit increased MEKK3 activity like that we have observed in CCM-deficient endocardial cells, and that changes in gene expression resulting from increased MEKK3 activity also underlie CCM disease pathogenesis. Future studies that test rescue of CCM formation in mice using either genetic or pharmacologic loss of MEKK3 pathway activity should be able to test this clinically important hypothesis.

EXPERIMENTAL PROCEDURES

Mice

Nfatc1^{Cre} (Wu et al., 2012), Ccm2$^{fl/fl}$ (Zheng et al., 2012), Pdcd10$^{fl/fl}$ (Chan et al., 2010), and Krit1$^{fl/fl}$(Mleynek et al., 2014) animals have been previously described. The ROSA26-YFP reporter line was obtained from Jackson Laboratories (#006148). Map3k3$^{fl/fl}$ animals were generated as shown in Figure S6. The University of Pennsylvania Institutional Animal Care and Use Committee approved all animal protocols.

Histology

Embryos and tissues were fixed in 10% formaldehyde overnight, dehydrated in 100% ethanol, and embedded in paraffin. Eight micrometer thick sections were used for H&E, Alcian blue, and immunohistochemistry staining. Klf2 in situ hybridization was performed as previously reported (Lee et al., 2006). The following antibodies were used for immunostaining: rat anti-Pecam (1:500, BD PharMingen), rabbit anti-Versican (1:200, Millipore), and rabbit anti-DPEAAE (1:200, Pierce-Antibodies).

Zebrafish Studies

Zebrafish were maintained and with approval of the Institutional Animal Care and Use Committee of the University of Pennsylvania. ccm2^{hi296} mutant zebrafish were obtained from the Zebrafish International Resource Center (ZIRC). i-fabp:GFP transgenic embryos in which the heart is fluorescently labeled were kindly provided by Dr. Michael Pack. The cardiac reporter zebrafish were created by transposon-based gene trap approach using the 192 base pair zebrafish I-FABP promoter (Her et al., 2004). Morpholino oligonucleotides were obtained from Gene Tools and were injected into the yolk of one-cell stage embryos at the indicated dosages and combinations. The morpholino sequences are described in the Supplemental Experimental Procedures.

Biochemical Studies

Biochemical studies of E10.5 Nfatc1^{Cre};Krit1$^{fl/fl}$ hearts were performed as previously described (Kleaveland et al., 2009; Zheng et al., 2010). The following

antibodies were used for immunonlotting: rabbit anti-Gapdh (1:5,000, Cell Signaling), rabbit anti-pERK5 (1:1,000, Cell Signaling), rabbit anti-Adamts5 (1:1,000, Abcam), and rabbit anti-DPEAAE (1:1,000, Pierce-Antibodies). Identification of BirA-MEKK3 interacting proteins is described in the Supplemental Experimental Procedures.

Endothelial Cell Studies

HUVECs (Lonza) were grown in endothelial basal medium supplemented with EGM-2 SingleQuots (Lonza). HUVECs were transfected overnight with 10 nM Ambion Silencer Select siRNA against Map3k3 (s8671, Invitrogen) or Ccm2 (s8671, Invitrogen) using siPORT Amine Transfection Agent (Invitrogen) according to the manufacturer's protocol. Seventy-two hours after transfection, total RNA was isolated using TRIzol Reagent (Invitrogen). cDNA was generated from 1 μg total RNA using Superscript III Reverse Transcriptase (Invitrogen). qPCR was performed in Power SYBR Green PCR Master Mix (Applied Biosciences) using primers described in the Supplemental Experimental Procedures.

Mouse Heart Explant Studies

Hearts from wild-type embryos on mixed background were collected at E10.5 and cultured in the presence of BIX02189 (5 uM) or DMSO for 24 hr on transwell filters as described previously (Lavine et al., 2005).

Statistics

p Values were calculated using an unpaired 2-tailed Student's t test, ANOVA, or chi-square analysis as indicated. The mean and SEM are shown in the bar graphs.

SUPPLEMENTAL INFORMATION

Supplemental Information includes Supplemental Experimental Procedures, seven figures, and one table and can be found with this article online at http://dx.doi.org/10.1016/j.devcel.2014.12.009.

REFERENCES

Akers, A.L., Johnson, E., Steinberg, G.K., Zabramski, J.M., and Marchuk, D.A. (2009). Biallelic somatic and germline mutations in cerebral cavernous malformations (CCMs): evidence for a two-hit mechanism of CCM pathogenesis. Hum. Mol. Genet. 18, 919–930.

Boulday, G., Blécon, A., Petit, N., Chareyre, F., Garcia, L.A., Niwa-Kawakita, M., Giovannini, M., and Tournier-Lasserve, E. (2009). Tissue-specific conditional CCM2 knockout mice establish the essential role of endothelial CCM2 in angiogenesis: implications for human cerebral cavernous malformations. Dis. Model. Mech. 2, 168–177.

Boulday, G., Rudini, N., Maddaluno, L., Blécon, A., Arnould, M., Gaudric, A., Chapon, F., Adams, R.H., Dejana, E., and Tournier-Lasserve, E. (2011).

Developmental timing of CCM2 loss influences cerebral cavernous malformations in mice. J. Exp. Med. *208*, 1835–1847.

Bouwmeester, T., Bauch, A., Ruffner, H., Angrand, P.O., Bergamini, G., Croughton, K., Cruciat, C., Eberhard, D., Gagneur, J., Ghidelli, S., et al. (2004). A physical and functional map of the human TNF-alpha/NF-kappa B signal transduction pathway. Nat. Cell Biol. *6*, 97–105.

Camenisch, T.D., Spicer, A.P., Brehm-Gibson, T., Biesterfeldt, J., Augustine, M.L., Calabro, A., Jr., Kubalak, S., Klewer, S.E., and McDonald, J.A. (2000). Disruption of hyaluronan synthase-2 abrogates normal cardiac morphogenesis and hyaluronan-mediated transformation of epithelium to mesenchyme. J. Clin. Invest. *106*, 349–360.

Chan, A.C., Li, D.Y., Berg, M.J., and Whitehead, K.J. (2010). Recent insights into cerebral cavernous malformations: animal models of CCM and the human phenotype. FEBS J. *277*, 1076–1083.

Chan, A.C., Drakos, S.G., Ruiz, O.E., Smith, A.C., Gibson, C.C., Ling, J., Passi, S.F., Stratman, A.N., Sacharidou, A., Revelo, M.P., et al. (2011). Mutations in 2 distinct genetic pathways result in cerebral cavernous malformations in mice. J. Clin. Invest. *121*, 1871–1881.

Chao, T.H., Hayashi, M., Tapping, R.I., Kato, Y., and Lee, J.D. (1999). MEKK3 directly regulates MEK5 activity as part of the big mitogen-activated protein kinase 1 (BMK1) signaling pathway. J. Biol. Chem. *274*, 36035–36038.

Deacon, K., and Blank, J.L. (1999). MEK kinase 3 directly activates MKK6 and MKK7, specific activators of the p38 and c-Jun NH2-terminal kinases. J. Biol. Chem. *274*, 16604–16610.

Dekker, R.J., van Soest, S., Fontijn, R.D., Salamanca, S., de Groot, P.G., VanBavel, E., Pannekoek, H., and Horrevoets, A.J. (2002). Prolonged fluid shear stress induces a distinct set of endothelial cell genes, most specifically lung Krüppel-like factor (KLF2). Blood *100*, 1689–1698.

Dekker, R.J., Boon, R.A., Rondaij, M.G., Kragt, A., Volger, O.L., Elderkamp, Y.W., Meijers, J.C., Voorberg, J., Pannekoek, H., and Horrevoets, A.J. (2006). KLF2 provokes a gene expression pattern that establishes functional quiescent differentiation of the endothelium. Blood *107*, 4354–4363.

Dupuis, L.E., McCulloch, D.R., McGarity, J.D., Bahan, A., Wessels, A., Weber, D., Diminich, A.M., Nelson, C.M., Apte, S.S., and Kern, C.B. (2011). Altered versican cleavage in ADAMTS5 deficient mice; a novel etiology of myxomatous valve disease. Dev. Biol. *357*, 152–164.

Gassmann, M., Casagranda, F., Orioli, D., Simon, H., Lai, C., Klein, R., and Lemke, G. (1995). Aberrant neural and cardiac development in mice lacking the ErbB4 neuregulin receptor. Nature *378*, 390–394.

Glading, A., Han, J., Stockton, R.A., and Ginsberg, M.H. (2007). KRIT-1/CCM1 is a Rap1 effector that regulates endothelial cell cell junctions. J. Cell Biol. *179*, 247–254.

Grego-Bessa, J., Luna-Zurita, L., del Monte, G., Bolós, V., Melgar, P., Arandilla, A., Garratt, A.N., Zang, H., Mukouyama, Y.S., Chen, H., et al. (2007). Notch signaling is essential for ventricular chamber development. Dev. Cell *12*, 415–429.

Groenendijk, B.C., Hierck, B.P., Vrolijk, J., Baiker, M., Pourquie, M.J., Gittenberger-de Groot, A.C., and Poelmann, R.E. (2005). Changes in shear stress-related gene expression after experimentally altered venous return in the chicken embryo. Circ. Res. *96*, 1291–1298.

Hale, A.T., Tian, H., Anih, E., Recio, F.O., 3rd, Shatat, M.A., Johnson, T., Liao, X., Ramirez-Bergeron, D.L., Proweller, A., Ishikawa, M., and Hamik, A. (2014). Endothelial Kruppel-like factor 4 regulates angiogenesis and the Notch signaling pathway. J. Biol. Chem. *289*, 12016–12028.

Her, G.M., Chiang, C.C., and Wu, J.L. (2004). Zebrafish intestinal fatty acid binding protein (I-FABP) gene promoter drives gut-specific expression in stable transgenic fish. Genesis *38*, 26–31.

Hilder, T.L., Malone, M.H., Bencharit, S., Colicelli, J., Haystead, T.A., Johnson, G.L., and Wu, C.C. (2007). Proteomic identification of the cerebral cavernous malformation signaling complex. J. Proteome Res. *6*, 4343–4355.

Huddleson, J.P., Srinivasan, S., Ahmad, N., and Lingrel, J.B. (2004). Fluid shear stress induces endothelial KLF2 gene expression through a defined promoter region. Biol. Chem. *385*, 723–729.

Jeansson, M., Gawlik, A., Anderson, G., Li, C., Kerjaschki, D., Henkelman, M., and Quaggin, S.E. (2011). Angiopoietin-1 is essential in mouse vasculature during development and in response to injury. J. Clin. Invest. *121*, 2278–2289.

Jenni, R., Rojas, J., and Oechslin, E. (1999). Isolated noncompaction of the myocardium. N. Engl. J. Med. *340*, 966–967.

Kleaveland, B., Zheng, X., Liu, J.J., Blum, Y., Tung, J.J., Zou, Z., Sweeney, S.M., Chen, M., Guo, L., Lu, M.M., et al. (2009). Regulation of cardiovascular development and integrity by the heart of glass-cerebral cavernous malformation protein pathway. Nat. Med. *15*, 169–176.

Lavine, K.J., Yu, K., White, A.C., Zhang, X., Smith, C., Partanen, J., and Ornitz, D.M. (2005). Endocardial and epicardial derived FGF signals regulate myocardial proliferation and differentiation in vivo. Dev. Cell *8*, 85–95.

Lee, J.S., Yu, Q., Shin, J.T., Sebzda, E., Bertozzi, C., Chen, M., Mericko, P., Stadtfeld, M., Zhou, D., Cheng, L., et al. (2006). Klf2 is an essential regulator of vascular hemodynamic forces in vivo. Dev. Cell *11*, 845–857.

Li, D.Y., and Whitehead, K.J. (2010). Evaluating strategies for the treatment of cerebral cavernous malformations. Stroke *41* (10, Suppl), S92–S94.

Li, L., Tatake, R.J., Natarajan, K., Taba, Y., Garin, G., Tai, C., Leung, E., Surapisitchat, J., Yoshizumi, M., Yan, C., et al. (2008). Fluid shear stress inhibits TNF-mediated JNK activation via MEK5-BMK1 in endothelial cells. Biochem. Biophys. Res. Commun. *370*, 159–163.

Liu, W., Draheim, K.M., Zhang, R., Calderwood, D.A., and Boggon, T.J. (2013). Mechanism for KRIT1 release of ICAP1-mediated suppression of integrin activation. Mol. Cell *49*, 719–729.

Mably, J.D., Mohideen, M.A., Burns, C.G., Chen, J.N., and Fishman, M.C. (2003). heart of glass regulates the concentric growth of the heart in zebrafish. Curr. Biol. *13*, 2138–2147.

Mably, J.D., Chuang, L.P., Serluca, F.C., Mohideen, M.A., Chen, J.N., and Fishman, M.C. (2006). santa and valentine pattern concentric growth of cardiac myocardium in the zebrafish. Development *133*, 3139–3146.

Maddaluno, L., Rudini, N., Cuttano, R., Bravi, L., Giampietro, C., Corada, M., Ferrarini, L., Orsenigo, F., Papa, E., Boulday, G., et al. (2013). EndMT contributes to the onset and progression of cerebral cavernous malformations. Nature *498*, 492–496.

McDonald, D.A., Shenkar, R., Shi, C., Stockton, R.A., Akers, A.L., Kucherlapati, M.H., Kucherlapati, R., Brainer, J., Ginsberg, M.H., Awad, I.A., and Marchuk, D.A. (2011). A novel mouse model of cerebral cavernous malformations based on the two-hit mutation hypothesis recapitulates the human disease. Hum. Mol. Genet. *20*, 211–222.

McDonald, D.A., Shi, C., Shenkar, R., Stockton, R.A., Liu, F., Ginsberg, M.H., Marchuk, D.A., and Awad, I.A. (2012). Fasudil decreases lesion burden in a murine model of cerebral cavernous malformation disease. Stroke *43*, 571–574.

Mleynek, T.M., Chan, A., Redd, M., Gibson, C.C., Davis, C., Shi, D.S., Chen, T., Carter, K.L., Ling, J., Blanco, R., et al. (2014). Lack of CCM1 induces hypersprouting and impairs response to flow. Hum Mol Genet. *23*, 6223–6234.

Nakamura, K., and Johnson, G.L. (2003). PB1 domains of MEKK2 and MEKK3 interact with the MEK5 PB1 domain for activation of the ERK5 pathway. J. Biol. Chem. *278*, 36989–36992.

Nakamura, A., and Manasek, F.J. (1981). An experimental study of the relation of cardiac jelly to the shape of the early chick embryonic heart. J. Embryol. Exp. Morphol. *65*, 235–256.

Nebreda, A.R., and Porras, A. (2000). p38 MAP kinases: beyond the stress response. Trends Biochem. Sci. *25*, 257–260.

Parmar, K.M., Nambudiri, V., Dai, G., Larman, H.B., Gimbrone, M.A., Jr., and García-Cardeña, G. (2005). Statins exert endothelial atheroprotective effects via the KLF2 transcription factor. J. Biol. Chem. *280*, 26714–26719.

Parmar, K.M., Larman, H.B., Dai, G., Zhang, Y., Wang, E.T., Moorthy, S.N., Kratz, J.R., Lin, Z., Jain, M.K., Gimbrone, M.A., Jr., and García-Cardeña, G. (2006). Integration of flow-dependent endothelial phenotypes by Kruppel-like factor 2. J. Clin. Invest. *116*, 49–58.

Riant, F., Bergametti, F., Ayrignac, X., Boulday, G., and Tournier-Lasserve, E. (2010). Recent insights into cerebral cavernous malformations: the molecular genetics of CCM. FEBS J. *277*, 1070–1075.

Roux, K.J., Kim, D.I., Raida, M., and Burke, B. (2012). A promiscuous biotin ligase fusion protein identifies proximal and interacting proteins in mammalian cells. J. Cell Biol. *196*, 801–810.

Sandy, J.D., Westling, J., Kenagy, R.D., Iruela-Arispe, M.L., Verscharen, C., Rodriguez-Mazaneque, J.C., Zimmermann, D.R., Lemire, J.M., Fischer, J.W., Wight, T.N., and Clowes, A.W. (2001). Versican V1 proteolysis in human aorta in vivo occurs at the Glu441-Ala442 bond, a site that is cleaved by recombinant ADAMTS-1 and ADAMTS-4. J. Biol. Chem. *276*, 13372–13378.

Serebriiskii, I., Estojak, J., Sonoda, G., Testa, J.R., and Golemis, E.A. (1997). Association of Krev-1/rap1a with Krit1, a novel ankyrin repeat-containing protein encoded by a gene mapping to 7q21-22. Oncogene *15*, 1043–1049.

Sohn, S.J., Li, D., Lee, L.K., and Winoto, A. (2005). Transcriptional regulation of tissue-specific genes by the ERK5 mitogen-activated protein kinase. Mol. Cell. Biol. *25*, 8553–8566.

Somekawa, S., Imagawa, K., Hayashi, H., Sakabe, M., Ioka, T., Sato, G.E., Inada, K., Iwamoto, T., Mori, T., Uemura, S., et al. (2012). Tmem100, an ALK1 receptor signaling-dependent gene essential for arterial endothelium differentiation and vascular morphogenesis. Proc. Natl. Acad. Sci. USA *109*, 12064–12069.

Stankunas, K., Hang, C.T., Tsun, Z.Y., Chen, H., Lee, N.V., Wu, J.I., Shang, C., Bayle, J.H., Shou, W., Iruela-Arispe, M.L., and Chang, C.P. (2008). Endocardial Brg1 represses ADAMTS1 to maintain the microenvironment for myocardial morphogenesis. Dev. Cell *14*, 298–311.

Stockton, R.A., Shenkar, R., Awad, I.A., and Ginsberg, M.H. (2010). Cerebral cavernous malformations proteins inhibit Rho kinase to stabilize vascular integrity. J. Exp. Med. *207*, 881–896.

Tatake, R.J., O'Neill, M.M., Kennedy, C.A., Wayne, A.L., Jakes, S., Wu, D., Kugler, S.Z., Jr., Kashem, M.A., Kaplita, P., and Snow, R.J. (2008). Identification of pharmacological inhibitors of the MEK5/ERK5 pathway. Biochem. Biophys. Res. Commun. *377*, 120–125.

Uhlik, M.T., Abell, A.N., Johnson, N.L., Sun, W., Cuevas, B.D., Lobel-Rice, K.E., Horne, E.A., Dell'Acqua, M.L., and Johnson, G.L. (2003). Rac-MEKK3-MKK3 scaffolding for p38 MAPK activation during hyperosmotic shock. Nat. Cell Biol. *5*, 1104–1110.

Vermot, J., Forouhar, A.S., Liebling, M., Wu, D., Plummer, D., Gharib, M., and Fraser, S.E. (2009). Reversing blood flows act through klf2a to ensure normal valvulogenesis in the developing heart. PLoS Biol. *7*, e1000246.

Villarreal, G., Jr., Zhang, Y., Larman, H.B., Gracia-Sancho, J., Koo, A., and García-Cardeña, G. (2010). Defining the regulation of KLF4 expression and its downstream transcriptional targets in vascular endothelial cells. Biochem. Biophys. Res. Commun. *391*, 984–989.

Weksler, B.B., Subileau, E.A., Perrière, N., Charneau, P., Holloway, K., Leveque, M., Tricoire-Leignel, H., Nicotra, A., Bourdoulous, S., Turowski, P., et al. (2005). Blood-brain barrier-specific properties of a human adult brain endothelial cell line. FASEB J. *19*, 1872–1874.

Whitehead, K.J., Plummer, N.W., Adams, J.A., Marchuk, D.A., and Li, D.Y. (2004). Ccm1 is required for arterial morphogenesis: implications for the etiology of human cavernous malformations. Development *131*, 1437–1448.

Whitehead, K.J., Chan, A.C., Navankasattusas, S., Koh, W., London, N.R., Ling, J., Mayo, A.H., Drakos, S.G., Jones, C.A., Zhu, W., et al. (2009). The cerebral cavernous malformation signaling pathway promotes vascular integrity via Rho GTPases. Nat. Med. *15*, 177–184.

Wu, B., Zhang, Z., Lui, W., Chen, X., Wang, Y., Chamberlain, A.A., Moreno-Rodriguez, R.A., Markwald, R.R., O'Rourke, B.P., Sharp, D.J., et al. (2012). Endocardial cells form the coronary arteries by angiogenesis through myocardial-endocardial VEGF signaling. Cell *151*, 1083–1096.

Yamamura, H., Zhang, M., Markwald, R.R., and Mjaatvedt, C.H. (1997). A heart segmental defect in the anterior-posterior axis of a transgenic mutant mouse. Dev. Biol. *186*, 58–72.

Yang, J., Boerm, M., McCarty, M., Bucana, C., Fidler, I.J., Zhuang, Y., and Su, B. (2000). Mekk3 is essential for early embryonic cardiovascular development. Nat. Genet. *24*, 309–313.

Zawistowski, J.S., Stalheim, L., Uhlik, M.T., Abell, A.N., Ancrile, B.B., Johnson, G.L., and Marchuk, D.A. (2005). CCM1 and CCM2 protein interactions in cell signaling: implications for cerebral cavernous malformations pathogenesis. Hum. Mol. Genet. *14*, 2521–2531.

Zhang, J., Rigamonti, D., Dietz, H.C., and Clatterbuck, R.E. (2007). Interaction between krit1 and malcavernin: implications for the pathogenesis of cerebral cavernous malformations. Neurosurgery *60*, 353–359, discussion 359.

Zheng, X., Xu, C., Di Lorenzo, A., Kleaveland, B., Zou, Z., Seiler, C., Chen, M., Cheng, L., Xiao, J., He, J., et al. (2010). CCM3 signaling through sterile 20-like kinases plays an essential role during zebrafish cardiovascular development and cerebral cavernous malformations. J. Clin. Invest. *120*, 2795–2804.

Zheng, X., Xu, C., Smith, A.O., Stratman, A.N., Zou, Z., Kleaveland, B., Yuan, L., Didiku, C., Sen, A., Liu, X., et al. (2012). Dynamic regulation of the cerebral cavernous malformation pathway controls vascular stability and growth. Dev. Cell *23*, 342–355.